Available online at www.sciencedirect.com

ScienceDirect

Procedia CIRP 58 (2017) 629 – 634

www.elsevier.com/locate/procedia

16th CIRP Conference on Modelling of Machining Operations

Method of hole shrinkage radial forces measurement in Ti6Al4V drilling

Johan Merzouki[a,c*], Gérard Poulachon[a], Frédéric Rossi[a], Yessine Ayed[b], Guillaume Abrivard[c]

[a] *LaBoMaP – Arts et Métiers ParisTech Cluny, Rue Porte de Paris, 71250 CLUNY, France.*
[b] *LAMPA - Arts et Métiers ParisTech Angers, 2 boulevard du Ronceray, 49035 ANGERS, France*
c Airbus Group Innovations - Centre Technocampus EMC2, Chemin du Chaffault, 44340 BOUGUENAIS, France.

* Corresponding author. Tel.: +33 6 15 44 36 50. *E-mail address:* johan.merzouki@ensam.eu

Abstract

This work deals with the phenomenon of hole shrinkage during Ti6Al4V drilling. Indeed, the shape and dimensions of the drilled hole, as well as the heat generated by the operation depend on this phenomenon which is caused by multiple factors, including the relaxation of internal residual stresses, thermal expansion and diverse thermomechanical loads applied to the workpiece and the tool. Nevertheless, the present study focuses only on the mechanical aspect and especially aims at showing the development of an innovative method to measure the radial forces induced by the hole shrinkage phenomenon.

Peer-review under responsibility of the scientific committee of The 16th CIRP Conference on Modelling of Machining Operations

Keywords: Drilling;.Force; Hole shrinkage.

1. Introduction

On account of the major economic and ecological stakes to which the aeronautic industry stakeholders had to react during the last decades, the composite mass percentage in aircrafts never stopped to increase and reached more than 50% in 2013 for the Airbus A350. Indeed, the aim always being to build lighter aircrafts, aluminum alloys (which represented more than 75% of the total mass in the 70') were gradually replaced by other materials which were considered to have more advantageous mechanical properties to weight ratios and especially by CFRP (Carbon Fiber Reinforced Plastic). Since the CFRP/titanium alloy pair demonstrates a better thermal and electrochemical compatibility compared to the CFRP/aluminum alloy pair, the use of titanium alloys in aircraft increased as well and reached 14% of the mass for the Airbus A350.

Therefore, many assembly cases are currently CFRP/Ti6Al4V hybrid stacks for which the goal is to be able to drill them in one shot, just as it was done for metal/metal stacks. Studies were carried out concerning hybrid stacks drilling and highlighted that the elevated temperatures during the Ti6Al4V drilling were mainly responsible for the non-fulfilment of aeronautical specifications and the quick tool wear. Based on these observations, the idea of using the cryogenic assistance in hybrid stacks drilling emerged: cooling down the cutting area by using liquid nitrogen instead of classic modes of lubrication and cooling.

The main goal of this research is to understand the causes of hole shrinkage which occurs in Ti6Al4V drilling and is believed to be the root cause of temperature increases. Indeed, once the causes and effects will be well identified, the understanding of the cryogenic assistance input will be within reach. Nevertheless, as explained in the abstract, the present study concentrates on the development of a method designed to measure radial forces induced by hole shrinkage in Ti6Al4V drilling and is only a step in the whole study.

Peer-review under responsibility of the scientific committee of The 16th CIRP Conference on Modelling of Machining Operations
doi:10.1016/j.procir.2017.03.226

2. State of the art

Even if there is an obvious lack of studies on cryogenic assistance applied to drilling operations, the concept of cryogenic assistance is known since decades and was tested several times on turning operations. Indeed, researchers like Hong and Ding [1] already confirmed its efficiency when it comes down to improving tool life in Ti6Al4V turning. Also, Courbon et al. [2] conducted tribological tests that confirmed the ability of the assistance to reduce the heat transmitted to the WC-Co cutting tools.

Nevertheless, in order to analyze and optimize the effects of the cryogenic assistance on the drilling of Ti6Al4V/CFRP stacks, one needs to understand why the operation is difficult. Fig. 1 summarizes the issues discussed in the literature when it comes down to drilling these stacks: for each material taken individually and for their combination in stack configuration.

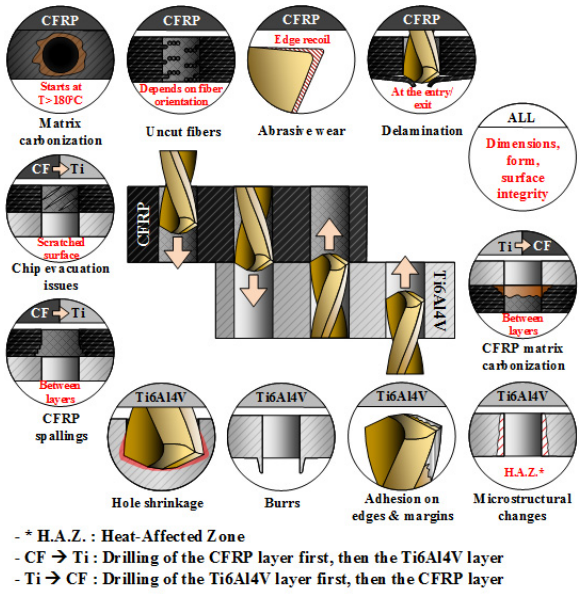

Fig. 1. Overview of the issues concerning Ti6Al4V/CFRP hybrid stacks drilling.

Regarding the stack in itself, studies showed that whatever the direction of drilling, the defects on the generated surface were mainly caused by difficulties linked to heat generation induced by the titanium alloy part. For instance, Dornfeld et al. [3] studied burr formation in Ti6Al4V drilling and concluded that its size was directly connected by the temperatures reached in the cutting zone during the exit of the drill. Cantero et al. [4] reached the same conclusions concerning burr formation and researched other issues as well, managing to link microstructural changes on the hole surface with temperature increases.

As shown on Fig. 2 Brinksmeier and Janssen [5] found out that even at constant cutting conditions throughout the machining, the diameter of the machined hole in a Ti6Al4V plate varies depending on the drilled depth. Moreover, the measured diameters are smaller than the diameter of the drill which reveals the existence of phenomena leading to shrinkage of the hole. As it happens, Bonnet [6] was able to highlight the major role of hole shrinkage on these temperature increases, yet he did not study the phenomenon in detail. In the end, hole shrinkage seems to be the root cause of the issues faced in titanium alloys drilling and by extension in Ti6Al4V/CFRP stacks, that is why it was chosen to orientate the study in this way.

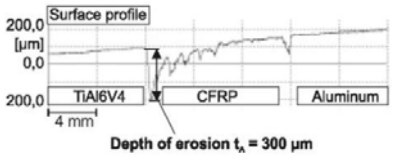

Fig. 2. Roughness profile of a hole machined in a Ti6Al4V/CFRP/Aluminum stack [5].

In practice, hole shrinkage in titanium alloys manifests itself as shown on Fig. 3. Indeed, while drilling the workpiece, the actual diameter of the drilled hole is ultimately smaller than the theoretical diameter of the hole which is supposed to be the diameter of the drill. Because of the back taper of the drill, this leads to a contact between the tool and the hole surface which height is directly linked to the hole shrinkage by the angle of the back taper. Consequently, the shrinkage induces two kinds of mechanical loads on the drill margins:

- Tangential loads, due to the friction between the hole surface and the margins. Those can be measured with usual means giving measurement of the torque. Obviously, this friction also has a role in heat generation.
- Radial loads, due to the shrinkage of the hole on the margins. Those cannot be measured by usual means and can only be estimated using unsure assumptions.

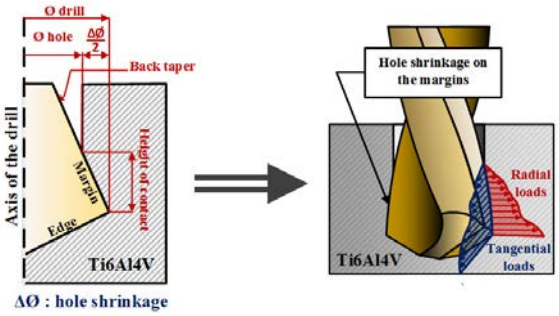

Fig. 3. Hole shrinkage and induced mechanical loads on the margins.

An in-depth study of the literature concerning hole shrinkage in Ti6Al4V drilling showed that this phenomena seems to be the result of the combination of several loads leading to strains in the tool and in the workpiece. Especially:

- Initial residual stresses relaxation in the workpiece;
- Thermal expansion and contraction in the workpiece and the tool;
- Elastic strains in the workpiece and the tool;
- Plastic strains in the workpiece;
- Residual stresses induced by the drilling in the workpiece.

Indeed, those phenomena were already highlighted and sometimes studied in the literature. For instance, as shown on Fig. 4, Bono and Ni [7] tried to predict the final dimensions and form of drilled holes in an aluminum alloy by developing a model taking into account the thermal expansion of the drill as well as the workpiece contraction.

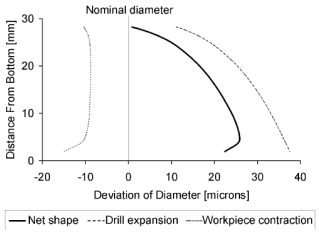

Fig. 4. Prediction of the final dimensions and form of a hole drilled in a aluminium 319 plate [7].

Also, Bonnet [6] identified two kinds of elastic deformations following the passage of the edge: one elastic springback due to the elimination of the mechanical load and one elastic strain due to the thermal loads on the hole surface. Nobre and Outeiro [8] determined induced residual stresses and strains due to drilling of Ti6Al4V alloy by using an experimental-numerical methodology. It allowed them to compute the induced strain relaxation that follows the operation and leads to a diameter change.

In every case, in order to understand hole shrinkage, it is necessary to measure the thermal and mechanical loads seen by the hole during its drilling, as well as their effects. Therefore, this paper aims to present the experiment conducted in order to determine the mechanical loads and especially the radial forces induced by hole shrinkage.

3. Experimental setup

The drilling tests were performed on a 3 axis DMG 85V CNC milling center. As shown on Fig. 5, the holes were made using ISCAR cutting tools which were composed of a SUMOCHAM holder, reference DCN 120-060-16-5D, and several indexable carbide heads, reference ICM 120 IC908, having 12 mm diameter, 140° tool tip angle, 1% back taper.

Fig. 5. Tool holder and indexable head, assembled and taken apart.

The goal of this experiment was to measure the radial forces caused by hole shrinkage during Ti6Al4V drilling. In order to get this information and as shown on Fig. 6, holes were drilled between two plates separated by a gap of 1 mm. One was attached to a KISTLER dynamometer (type 9257B, 3 components) and the other was attached to a replica of this dynamometer, thus allowing to measure forces in the plane perpendicular to the drill axis. Moreover, torque and feed force were measured using a KISTLER rotating dynamometer (type 9123C, 4 components).

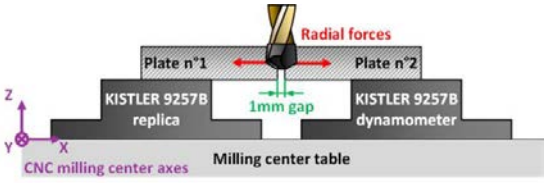

Fig. 6. Principle of the experiment aiming to measure radial forces.

The angular position of the edges was measured by bypassing the signals coming from the spindle encoder. As shown on Fig. 7, the angular position of reference was chosen in such a way that $\theta_{edge} = 0°$ corresponded to the angle where the major cutting edges were parallel to the X-axis of the CNC milling center.

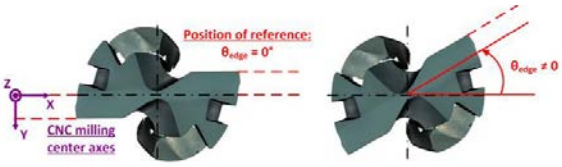

Fig. 7. Angular position of reference.

The drilling tests were conducted under dry cutting conditions with a cutting speed (v_c) and a feed (f) equal to 30 m/min and 0,08 mm/rev respectively.

Afterwards, this particular experiment will be referred to as the “bi-plates case” as opposed to the usual way of measuring efforts on one plate fixed on one dynamometer which will be referred to as the “mono-plate case”.

4. Results and discussion

4.1. Results expressed on a global scale

First of all, the forces measured using the KISTLER type 9257B 3-components dynamometer were analyzed on a global scale. Fig. 8 shows the results for the force in the milling center X-axis direction Fx as well as a zoom on a few revolutions of the drill and a zoom on the exit of the drill. It allowed to check that when the drill rises back up and exits the plate, the measured force goes back to zero, proving that there are no remaining loads on the plate. Also, it allowed to check that the oscillations are indeed corresponding to the edges passing by computing the frequency of the signal and comparing it to the frequency of the drill’s revolution. These

observations are also valid for the forces in the milling center Y-axis direction.

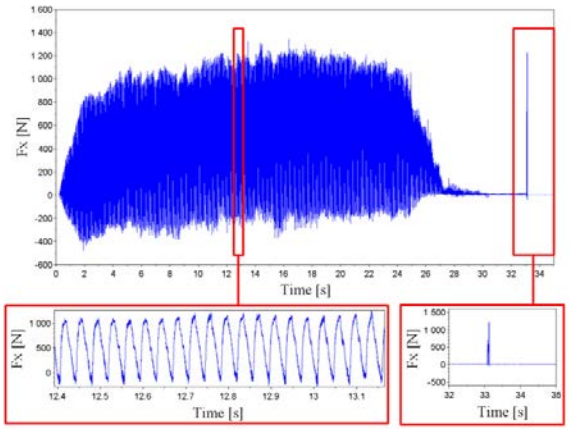

Fig. 8. Fx as a function of time in the bi-plates case.

Then, as the bi-plates case differs from the usual mono-plate case, it was critical to check the differences between them. In order to identify and quantify these, the feed force and cutting torque were measured by using a KISTLER type 9123C rotating 4-component dynamometer and the results were confronted with measurements of a drilling in the mono-plate case.

Thus, Fig. 9 shows the comparison on the feed force F_z for a drilling operation at v_c = 30 m/min and f = 0,08 mm/rev. In both cases the results were filtered using a Butterworth filter (order = 4, cutoff frequency = 10 Hz) in order to have a better view of the global evolution without being bothered by the high-frequency phenomena. The difference in feed force is significant, the maximum in the mono-plate case being 1643 N whereas it is 1125 N in the bi-plates case. This experimental setup leads to a feed force which is 31,5 % lower than in the usual case. This can be explained by the fact that in the bi-plates case the center of the drill has no matter to cut.

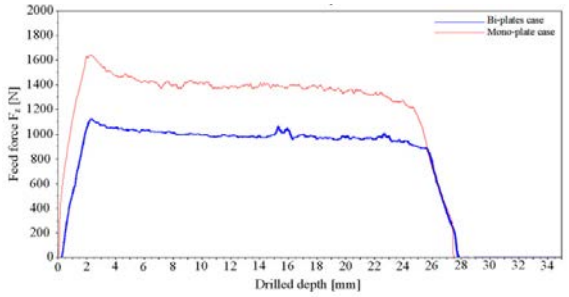

Fig. 9. Feed force F_z comparison between the bi-plates case and the mono-plate case.

Fig. 10 shows the comparison on cutting torque M_z in the exact same conditions. The results were filtered in the same way that the feed force was. The differences in values are also significant for the torque, the maximum in the mono-plate case being 6,8 N.m whereas it is 6 N.m in the bi-plates case which is 11,7 % lower and can also be explained by the gap between the two Ti6Al4V plates. In a consistent manner, the deviation between both configurations is smaller in the case of torque because the main contribution to feed force is due to the drill web whereas the main contribution to torque is due to the major cutting edges.

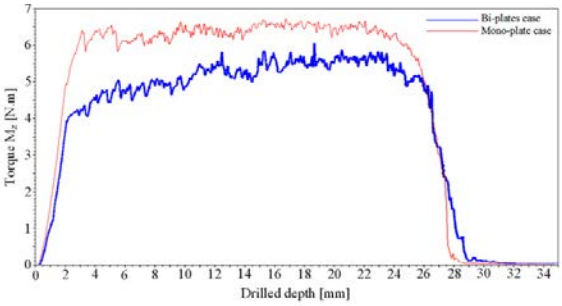

Fig. 10. Cutting torque M_z comparison between the bi-plates case and the mono-plate case.

4.2. Polar representations of the cutting forces and torque

Without an in depth-study of the measured signals, it is virtually impossible to get the information of interest which is the radial forces applied to the drill. That is why each revolution of the drill was processed separately and the cutting forces and torque were expressed in function of the angular position of the edges θ_{edge}. Fig. 11 shows these polar representations of F_x, F_y and M_z for one complete revolution of the drill. The chosen revolution corresponds to a drilled depth between 13,28 mm and 13,36 mm where the edges and margins of the indexable head have already fully entered in between the two plates.

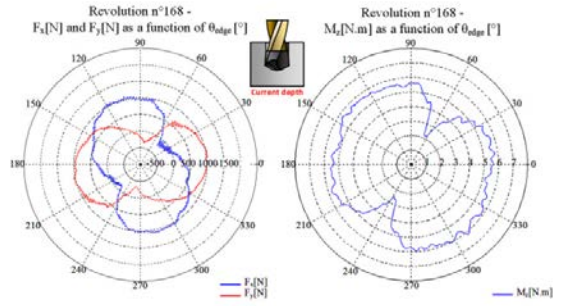

Fig. 11. Fx, Fy and Mz as a function of θ_{edge} for the 168th revolution of the drill.

Concerning the forces in the X and Y directions, since the coordinate system is fixed, the data is difficult to explain in this state and for only one revolution. Nevertheless, the form

of these signals is particular and contains two minima and two maxima for one complete revolution. The cutting torque M_z is easier to interpret since its measure does not depend on the coordinate system and is synced with θ_{edge}. Here, the minima at around 60° and 240° correspond to the time when the edges are exiting one plate before entering the other. The rest of the signal can be considered stable between 90° and 210° and between 270° and 30°. It means that in order to compute radial and tangential forces, F_x and F_y should be taken in between these angles where the cutting operation is stable.

The remarks made in the previous paragraph are only true for one revolution and the angles where the minima and maxima occur actually change during the drilling and are linked to the geometry of the tool. Indeed, these angles evolve because the parts of the cutting edge and margins in contact with the machined material are changing throughout the drilling. Therefore, theoretical angular ranges of minimum and maximum contact between the drill and the plates were determined using an algorithm developed on SCILAB for which the input data consisted in the coordinates of each point on the edges and the margins, previously determined using a CAD model of the indexable head.

As a result, Fig. 12 allows to see where the minima of cutting torque M_z happen throughout the whole operation, theoretically and experimentally. The same procedure was applied for the maxima, but since the ranges of maximum contact between the tool and the plates are wider, the experimental determination of θ_{edge} where maxima happen gave scattered results which are difficult to compare to the theoretical ranges.

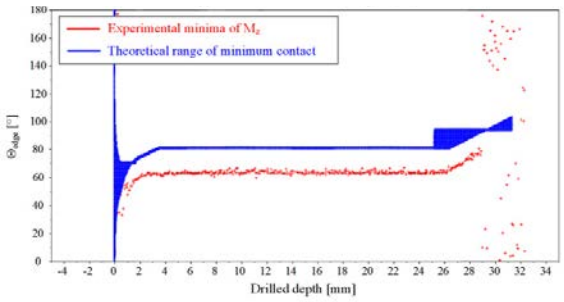

Fig. 12. Experimental and theoretical θ_{edge} for which the minima of M_z happen as a function of drilled depth.

Nevertheless, this approach allowed to have a global vision of the changes throughout the drilling as well as explaining it with a theoretical approach. More importantly, it led to the detection of an unidentified issue with the chain of measurement which was responsible in this case for an offset of 19° between θ_{edge} and the torque measurements. Indeed, this offset had to be taken into account for the local approach used in the next section.

4.3. Computation of radial and tangential forces

The interest of this experiment was to measure the radial forces which are not accessible by usual means. In order to obtain this information, the last step is to compute the radial and tangential forces from F_x and F_y. Since the orientation of radial and tangential forces is varying along the margins due to the helix angle, the analysis had to be carried out at a local scale.

To do so, the variations of F_x, F_y and M_z during the exit of the tool were extracted by taking a mean value between θ_{edge} = 1° and θ_{edge} = - 1° for each revolution of the drill. While this choice was made arbitrary, this angular range ensures that the margins are entirely in contact with the surface of the hole. Since the feed f is of 0,08 mm/rev, the extracted values correspond to the contribution of F_x, F_y and M_z for margin portions measuring 0,08 mm of height. The interest of extracting M_z is to be able to compute the tangential contributions ΔF_t using two different methods: by projecting each contribution ΔF_x and ΔF_y in the local radial-tangential basis and by taking half of each contribution ΔM_z divided by the distance between the axis of the drill and the margins.

Fig. 13 shows the variations of M_z as a function of height on the margins, from 0 mm to the height of contact H = 1,84 mm which is marking the end of the contact between the margins and the hole walls. Fig. 13 also shows the polynomial regression used to compute the local contributions ΔM_z. The chosen regression consists of a second order polynomial for which the axis of symmetry was constrained to coincide with x = H in order to obtain smooth results for the computed ΔM_z and to ensure that these ΔM_z tends towards zero at the end of the contact between the margins and the hole. The exact same treatment was applied to F_x and F_y, allowing to compute ΔF_x, ΔF_y and ΔM_z using the obtained equations.

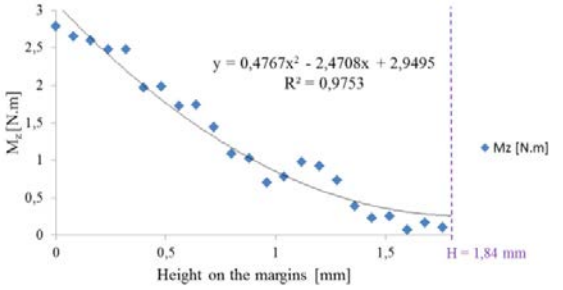

Fig. 13. M_z as a function of height on the margins during the exit of the drill

Fig. 14 shows the results of the computation of ΔF_r and ΔF_t. As discussed earlier, ΔF_t was determined using two sources, thus allowing to check the coherence of the results obtained using ΔF_x and ΔF_y.

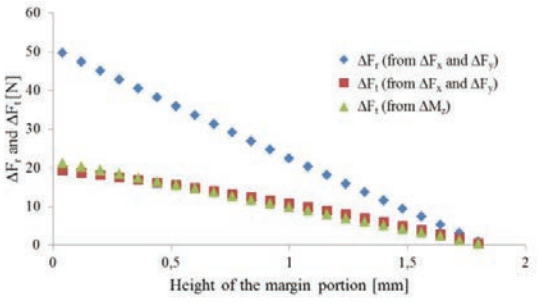

Fig. 14. Radial and tangential contributions for each margin portion in contact with the hole wall

Using the data obtained and knowing the width of the margins, it is possible to compute the repartition of normal and shear stress on the margins. Since these physical quantities are only linked by the surface of a portion, they follow the same evolution, the maximum normal stress being of 729 MPa whereas the maximum shear stress is of 283 MPa. Moreover, Fig. 15 shows that by dividing ΔF_t by ΔF_r, the data allows to see the evolution of the apparent friction coefficient between the margins and the workpiece. The coefficient evolves from 0,39 to 0,55 between the moment when the first margin portion exits the hole and the moment when the last portion does. The fact that the coefficient increases is consistent with the tribological tests carried out by Bonnet [6] for which the pin he used was rubbing on the same surface several times in an attempt to approach the same conditions as the friction between the margins and the workpiece.

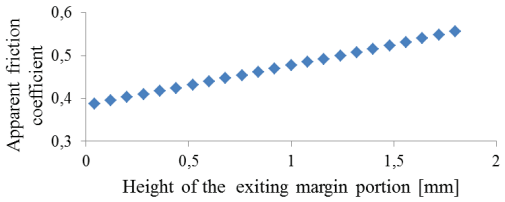

Fig. 15. Evolution of the apparent friction coefficient between the margins and the hole wall

5. Conclusions

This work has permitted to develop an innovative method to measure radial forces induced by hole shrinkage in Ti6Al4V drilling. The computation of local radial and tangential forces on the margins also allowed to determine the normal and tangential stresses applied on each portion, as well as the evolution of the apparent friction coefficient between the workpiece and the margins while the drill is exiting the hole. By extension, progress was made towards the knowledge of the thermomechanical loads caused by this shrinkage phenomenon.

Consequently, keeping the goal of understanding the phenomenon of hole shrinkage in mind, other tests are to be made, especially ones for which temperatures are measured in the tool and the workpiece but also ones where displacements are measured. Then, using the acquired data and knowledge, a FEM model is to be developed in order to simulate the hole formation.

Once the dry cutting condition will be well studied, the cryogenic assistance input will be added in order to understand exactly what effects it can have on hole shrinkage.

Acknowledgements

The Ti6Al4V plates and cutting tools used in this work were provided by AIRBUS GROUP INNOVATIONS and ISCAR respectively. The author gratefully acknowledges their support.

References

[1] Hong, S.Y., Ding, Y., 2001. Cooling approaches and cutting temperatures in cryogenic machining of Ti-6Al-4V. International Journal of Machine Tools and Manufacture 41, p. 1417–1437.
[2] Courbon, C., Pusavec, F., Dumont, F., Rech, J., Kopac, J., 2013. Tribological behaviour of Ti6Al4V and Inconel718 under dry and cryogenic conditions—Application to the context of machining with carbide tools. Tribology International 66, p. 72–82.
[3] Dornfeld, D.A., Kim, J.S., Dechow, H., Hewson, J., Chen, L.J., 1999. Drilling Burr Formation in Titanium Alloy, Ti-6AI-4V. CIRP Annals - Manufacturing Technology 48, p. 73–76.
[4] Cantero, J.L., Tardío, M.M., Canteli, J.A., Marcos, M., Miguélez, M.H., 2005. Dry drilling of alloy Ti–6Al–4V. International Journal of Machine Tools and Manufacture 45, p. 1246–1255.
[5] Brinksmeier, E., Janssen, R., 2002. Drilling of Multi-Layer Composite Materials consisting of Carbon Fiber Reinforced Plastics (CFRP), Titanium and Aluminum Alloys. CIRP Annals - Manufacturing Technology 51, p. 87–90.
[6] Bonnet, C., 2010. Understanding of cutting mechanisms involved during the dry drilling of Ti6Al4V/CFRP stacks. PhD Thesis. Arts et Métiers ParisTech Cluny campus, defended on 12/10/2010. 207 pages.
[7] Bono, M., Ni, J., 2001. The effects of thermal distortions on the diameter and cylindricity of dry drilled holes. International Journal of Machine Tools and Manufacture 41, p. 2261–2270.
[8] Nobre, J.P., Outeiro, J.C., 2015. Evaluating Residual Stresses Induced by Drilling of Ti-6Al-4V Alloy by Using an Experimental-numerical Methodology. Procedia CIRP, 15th CIRP Conference on Modelling of Machining Operations (15th CMMO) 31, p. 215–220.
[9] Valiorgue, F., Rech, J., Hamdi, H., Gilles, P., Bergheau, J.M., 2012. 3D modeling of residual stresses induced in finish turning of an AISI304L stainless steel. International Journal of Machine Tools and Manufacture 53, p. 77–90.